Raman Spectroscopic and Computational Study of Hydrogen Bond Interactions between Guanidine Hydrochloride, Trimethylamine N-oxide (TMAO), Urea, and Water

by
Andrew Kamischke

A thesis submitted to the faculty of the University of Mississippi in partial fulfillment of the requirements of the Sally McDonnell Barksdale Honors College

Oxford
May 2018

Approved by

_____
Advisor: Professor Nathan Hammer

_____
Reader: Professor Susan Pedigo

_____
Reader: Professor Murrell Godfrey

ACKNOWLEDGEMENTS

The completion of this thesis and all the research done throughout my undergraduate studies was only possible through the guidance and support of many individuals. I would like to first thank Dr. Nathan Hammer for accepting me into his research group and giving me the resources and guidance for completing my research and preparing me for graduate school. I would also like to specifically thank April Steen and Dr. Louis McNamara for always being there to help me when I needed it along with the rest of the Hammer group for supporting me and my research. My research was also made possible by the National Science Foundation under grants CHE-1532079 & OIA-1539035. My thanks also extend to the Sally McDonnell Barksdale Honors College for the opportunity to take more challenging and stimulating class along with helping pay for my research endeavors. I would not have been able to finish without the loving support and encouragement from my friends and family. When I thought I was going to quit and not make it my family and friends were there to push me to the finish line. Because of the support from the above individuals I will be continuing my educational career by pursing a PhD in Chemistry at George Washington University in Washington D.C.

ABSTRACT

ANDREW DANIELSEN KAMISCHKE: Raman Spectroscopic and Computational Study of Hydrogen Bond Interactions between Guanidine Hydrochloride, Trimethylamine N-oxide (TMAO), Urea, and Water

(Under the direction of Dr. Nathan Hammer)

Proteins are broken down in the body and produce water, CO_2, and ammonia as by-products. Ammonia is toxic to cells, making it a priority to be excreted. Urea is the key route for the transportation of ammonia out of the body and is the main component of urine. Guanidine is another important nitrogen-containing molecule that is structural like urea and plays important biological roles in the stabilization of proteins. Guanidine hydrochloride and Urea are known to denature proteins and this functionality continues to be a topic of great interest. Urea and guanidine contain many hydrogen bonding sites and interactions with water are important to their biological functionality and their abilities to affect protein stability. Trimethylamine N-oxide (TMAO) is known to counteract the effects that urea and guanidine hydrochloride have at destabilizing proteins. Here, we use Raman spectroscopy to study how urea, guanidine hydrochloride, and TMAO affect the hydrogen bonded network of water both in solution at room temperature and in a frozen crystal state. The experiment confirmed previous research that showed a blue shift in the HNH bending region of urea when TMAO was added. Raman spectra of guanidine hydrochloride and TMAO was found to have two different blue shifts in the HNH bending region. Another perspective result for future research is that the low temperature Raman spectra of urea water was found show multiple peaks.

TABLE OF CONTENTS

LIST OF FIGURES, TABLES, AND EQUATIONS

LIST OF ABBREVIATIONS

Δ	Change in
α	Alpha
β	Beta
γ (Lambda)	Wavelength (m)
v (nue)	Frequency of the incident photon
v_1 $(\text{nue})_1$	Shift in frequency
c	Speed of light in a vacuum $(\sim 3.00 * 10^8 \frac{m}{s})$
CCD	Charge-Coupled Device
cm	Centimeters
cm^{-1}	Wavenumbers
DI	Deionized
E	Energy
EM	Electromagnetic
Gdn-HCl	Guanidine Hydrochloride
gr	Grating
h	Planck's constant $(6.626 * 10^{-3} \ \frac{J}{s})$
HPLC	High performance liquid chromatography
IR	Infrared
Laser	Light amplification by stimulated emission of radiation
m	Meters
nm	Nanometers
RUNS	Raman under Nitrogen spectroscopy
SERS	Surface enhanced Raman spectroscopy
TCS	Temperature control stage
TMAO	Trimethylamine N-oxide
UV-vis	Ultraviolet-visible
YAG	Yttrium Aluminum Garnet

Chapter 1: Introduction

1.1 Bonding

1.1.1 Overview

Chemical bonds are all around us and are the glue that holds different atoms together. Atoms are made up of particles of different charges that are located at different areas within the atom. The nucleus contains neutral particles, neutrons, and positive particles, protons. The final particle found in an atom is a negative species called an electron that orbits around the nucleus. The positive portion of an atom is attracted to the negative portion of another atom. When these interactions result in a net reduction of the potential energy of the particles, a bond is formed. The three broad categories of these intramolecular interactions are ionic, covalent, and metallic. Intramolecular forces occur within a molecule like the white and red bond between hydrogen and oxygen in **Figure 1.1.1.1.** The other type of bonding occurs between two molecules like the yellow dashed bond between the two water molecules in **Figure 1.1.1.1**. The intermolecular forces are weaker than intramolecular forces and are useful in determining physical properties of a compound like its melting point and boiling point. There are many different types of intermolecular forces including: ion-dipole, hydrogen bonding, dipole-dipole, ion-induced dipole, dipole-induced dipole, and London dispersion forces (LDF) [1]

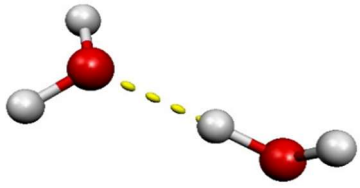

Figure 1.1.1.1: Intramolecular and Intermolecular bonding

1.1.2 Hydrogen Bonding

Hydrogen bonding is a special type of intermolecular interactions and is important in everyday life. Hydrogen bonding is not as strong as intramolecular forces like ionic and covalent bonds; however, it is known to be one of the strongest intermolecular force. To be able to understand what hydrogen bonding is, you must first understand some common notation. A hydrogen bond can be described by the notation X—H …Y. In this depiction X and Y are both electronegative elements. The hydrogen donor is X whereas the hydrogen accept is Y. The element Y also usually contains one or more lone pairs. The most well-known case of hydrogen bonding occurs when X and Y are of the following elements: fluorine, oxygen, or nitrogen. The acronym FON is often given to remember what elements exhibit hydrogen bonding. Other elements are known to exhibit hydrogen bonding like carbon; however the strength of the hydrogen bond with Carbon is much weaker than the ones listed above. [2] When a hydrogen bond occurs, there is a charge transfer from the proton acceptor to the proton donor. The charge transfer weakens the X—H bond causing the bond length to increase because of the weaker attraction forces. The resulting bond elongation is shown to cause a decrease in the vibrational frequency. A shift to lower frequency is associated with a lower energy and is often denoted as a red shift. When the vibrational frequency increases causing the energy to increase, a resulting blue shift is denoted. [2, 3]

1.2 Osmolytes

Osmolytes are an important category of molecules whose main function is the regulation of water in both intracellular and extracellular. There are many different types of osmolytes including free amino acids, polyhydric alcohols, and combinations of

methylamines. Within those different classes the three osmolytes that are of the most interest are urea, guanidine hydrochloride, and trimethylamine N-oxide. [4, 5]

Osmolytes are also known to interact with proteins and their structural dynamics. There are two different ways in which osmolytes may interact with a protein. Osmolytes may either interact in a positive manner pushing towards the folded state or negatively by pushing towards the unfolded state. The way in which these interaction occur is under much debate; however, it occurs without the making or breaking of covalent bonds. [6]

1.2.1 Urea

1.2.1.1 Structure and Properties

Urea has a molecular formula of CH_4N_2O and has a planar geometry in the crystalline form. It has a pH around neutral at 7.2 and it is highly soluble in water at 545g/L. Solid urea is a white crystal or powder.[7] **Figure 1.2.1.1.1** is a microscopic picture of crystalline urea using the CCD camera on the Raman spectrometer.

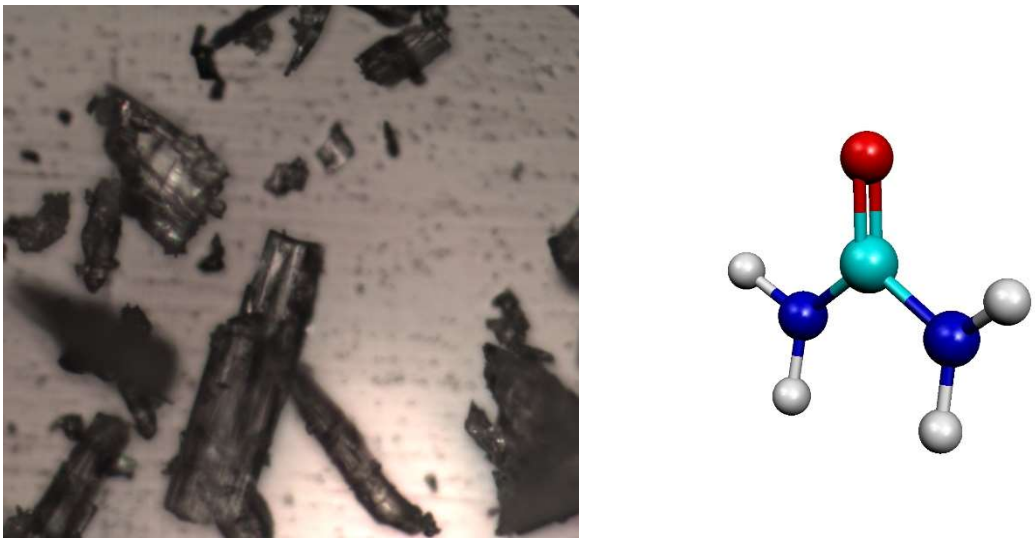

Figure 1.2.1.1.1: Photograph of solid urea (left) and molecular geometry (right)

1.2.1.2 Role

Urea has been studied for many years and was the first organic molecule to be synthesized.[8] Urea has many important roles in nature with the most notable being used for the removal of nitrogenous waste in living things. Nitrogenous waste is usually in the form of ammonia that is part of the backbone structure in amino acids. The way in which urea is used to accomplish that task is dependent upon the organism being studied. Birds and reptiles excrete their ammonia in the form of uric acid. Uric acid is a heterocyclic molecule with a chemical formula of $C_5H_4N_4O_3$. Organism that convert their waste into uric acid are known as uricotelic. Humans and most terrestrial organism excrete nitrogenous waste in the form of urea and are known as ureotelic. The process to make urea is called the urea cycle and is predominantly done in the liver. The cycle takes place in both the mitochondrial matrix and the cytosol within in the liver. Once free ammonium is converted to urea it travels through the blood and into the kidneys where it is finally excreted in the urine. Urea makes up the largest percentage of organic compounds in the urine. Urea is also a denaturant or chaotropic agent and that characteristic is of importance to this research. [9]

1.2.2 Guanidine Hydrochloride

1.2.2.1 Structure and Properties

Guanidine hydrochloride is a strong organic base with a molecular formula of CH_5N_3-HCl. Guanidine hydrochloride has a pH of 13.6 causing it to dissociate in physiological pH in the guanidinium form that contains an extra hydrogen along with having an overall charge of plus 1. The resulting compound at physiological pH has three resonance structure sharing the double bond and the overall charge of the molecule. [10, 11] **Figure 1.2.2.1.1** is a microscopic image of guanidine hydrochloride using the CCD

camera on the Raman spectrometer. Guanidine hydrochloride and guanidinium are used synonymously to describe the same structure. For this thesis guanidine hydrochloride will be used to describe this compound in all settings and will be abbreviated as gdn-HCl.

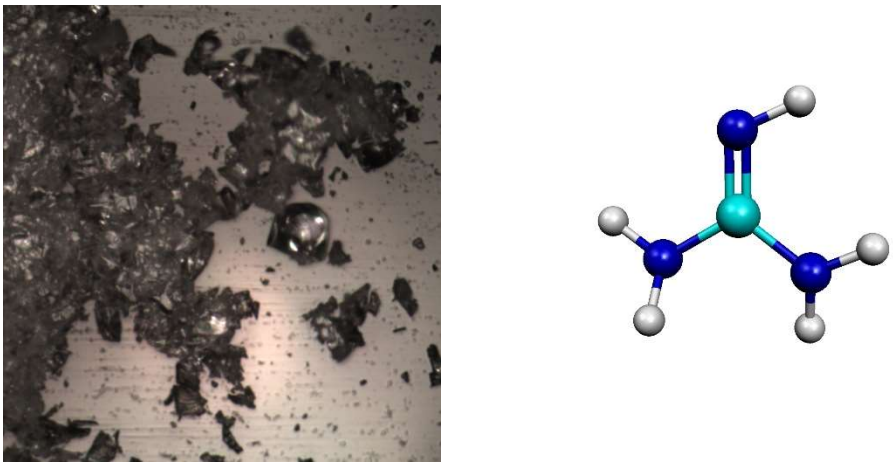

Figure 1.2.2.1.1: Photograph of solid guanidine hydrochloride (left) and molecular geometry (right)

1.2.2.2 Role

Guanidine hydrochloride has a few uses within organisms. Like urea, gdn-HCl can be found in the urine as a by-product of protein metabolism. On the medical side, gdn-HCl can be used to treat myasthenia which is a rare autoimmune disease that causes muscle weakness and the breakdown of communication between nerves and the muscles. It does this by fixing and increasing the release of the neurotransmitter, acetylcholine, after a nerve impulse. Another use of gdn-HCl is as a fluorescent tag or probe in HPLC. The characteristic that is of most importance for this research is that it is also a chaotropic compound. It causes proteins and other macromolecules to denature.

1.2.3 Trimethylamine N-oxide

1.2.3.1 Structure and Properties

Trimethylamine N-oxide also referred to as TMAO, has a chemical formula of C_3H_9NO. TMAO has an IUPAC name of N,N-dimethylmethanamine oxide and is a colorless solid at room temperature. TMAO has a solubility of 454 mg/mL in water. It has a net neutral charge; however, there is a positive charge on the Nitrogen and a negative charge on the Oxygen. [12]

1.2.3.2 Role

TMAO is commonly found in tissues of marine organisms and humans. In marine organisms it is used to protect against changes in salinity, temperature, hydrostatic pressure, and high amounts of urea. TMAO has many different roles in humans and other terrestrial organisms. It has recently been associated with cardiovascular disease in humans. TMAO's role in stabilizing proteins, kosmotropic agent, and causing them to fold back into their native state is of most importance for this research. [13] **Figure 1.2.3.2.1** is a microscopic image of solid TMAO using the CCD camera from the Raman spectrometer.

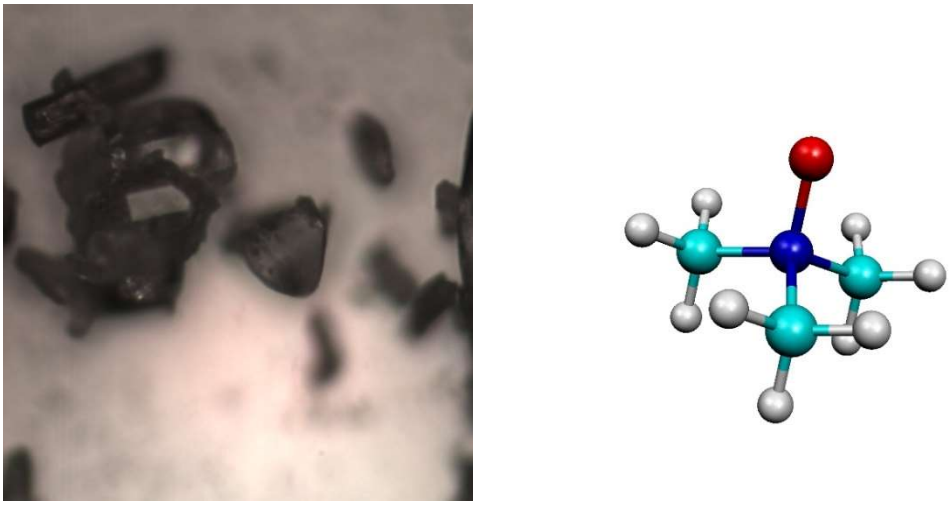

Figure 1.2.3.2.1: Photograph of solid TMAO (left) and molecular geometry (right)

1.3 Protein Synthesis and Degradation

1.3.1 Overview

Proteins are macromolecules that make up a large percentage of living things. They are crucial in many different biological process including movement, transportation and storage of molecules, provide mechanical support, immune protection, control growth, and many other functions. Proteins have many important attributes that enable them to have such a vast range of function. [9, 14] They have two major states or conformations that exist in nature; native and non-native. Native proteins are those that are folded and packaged tightly with their non-polar groups positions in the interior getting as far away from water as possible. On the other side is the non-native proteins that are prone to aggregation and unwanted interactions because their hydrophobic groups are no longer tucked away in the interior of the protein. The hydrophobic groups are then free to interact with water and other hydrophobic molecules affecting the intended purpose of the protein. The non-native structure is common in the body and is needed for important biological processes including protein synthesis, transportation through membranes, and for degradation. The downside occurs when the non-native structure is formed during times when it is supposed to be in the native state. [15]

1.3.2 Synthesis

Proteins are created from basic building blocks called amino acids that all contain the same backbone and vary by their substituents. There are four main structures associated with proteins: primary, secondary, tertiary, and quaternary. The primary structure is a one-dimensional structure of the sequence of amino acids and occurs after translation. The secondary structure is a result of the folding of the primary structure on to its self by means of α-helix and β-sheets. The tertiary structure is the three-dimensional structure created by

the folding of the secondary structure. The final possible structure is the quaternary structure that results from different tertiary subunits coming together to form a large assembled subunit. A common example of quaternary structure is the oxygen binding protein of red blood cells, hemoglobin. [9]

1.3.3 Degradation

Proteins may become degraded or pushed into their non-native states by many ways. There is a mechanical way in which one can physically unfold a protein using special optical tweezers. Proteins can also become denatured by thermal means along with by chemical changes from pH or the introductions of denaturants. [16] The use of denaturants is of the most importance for this study. The mechanism in which chemical denaturation occurs has baffled the scientific community. The two proposed ways is that either the denaturant directly interacts with the protein causing it to unfold [17-19] or that the denaturant interacts with water weakening the water structure which indirectly causes the protein to unfold. The weakened water structure occurs when the denaturant hydrogen bonds with water causing water to have less available bonding sites to contain the protein into its native state. [20-22] There are also those who believe that denaturation occurs as a result of a combination of the two theories. [23]

Urea begins to denature proteins after 8M. From a theoretical model, they determined that increasing concentrations of denaturants can cause sharp phase transitions of the native molecule to denature states because the denaturant solutions favorably solvate the nonpolar groups in the denatured state. Gdn-HCl was found to be a more effective denaturant at lower concentrations than urea at around 6M. Free energy should depend approximately

linearly on denaturant concentration for either gdn-HCl or urea over the typical experimentally accessible ranges. [24]

1.4 Previous Research

The topic involving protein denaturation and renaturation regarding osmolytes has baffled the scientific community. There are many articles that show the results of specific proteins with the addition of a particular denaturant like urea or gdn-HCl [17, 25, 26]. These types of article just show the result of the addition of different osmolytes and not what happens on the microscopic level. There are a few different reasons that have been studied in the literature. There is research that suggest that the interactions are a result of hydrophobic interactions and those that are induced by hydrogen bonding. [17]

One article concluded that when urea is placed in water, urea will hydrogen bond with water rather than create a urea dimer.[20] Another article found that the hydrogen bonds between urea and water were weaker than those between water and water. This causes urea to strengthen the water structure in the form of hydrogen bond energies leading to urea directly interacting with the protein.[18] Unlike urea and gdn-HCl, TMAO has been found to strengthen hydrogen bonds networks causing proteins to conform to their folded native state. [19]

The current research of the project is a continuation of previous research in the Hammer research group involving noncovalent interactions between different osmolytes in various environments. The first study was an analysis of noncovalent interactions between trimethylamine N-oxide and water. One of the conclusions from the research was that TMAO will create a cluster of three waters for every TMAO molecule when in

solution. The three water molecules are all bonded to the oxygen on TMAO and it was determined by comparing theoretical data with computational data. [27]

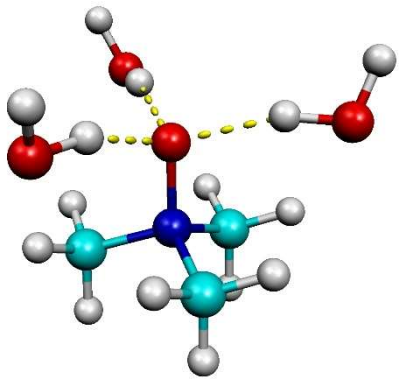

Figure 1.4.1: Molecular structure of TMAO in solution[27]

The next study expanded on the interaction of TMAO with water and looked at how TMAO interacts with various other solvents including methanol, ethanol, and ethylene glycol. The different solvents all were shown to interact directly with the oxygen atom on TMAO leaving the methyl groups on TMAO unchanged. From that it was proposed that the interactions with the oxygen on TMAO causes it to have its osmolyte features. Hyperconjugation was found with both TMAO and the solvents used and resulted with a charge transfer causing a blue shift in TMAO's C—H stretching mode. [28]

The most recent research that is most useful for this research involved the study of the noncovalent interaction between TMAO, urea, and water. The research was able to show strong agreement between experimental data and theoretical data suggesting that the theoretical structures are what occurs or is close to the actual arrangement. Because the theoretical graph matched the experimental graph, the different vibrational modes were

able to be determined. It was found that there was a blue shift, **Figure 1.4.2**, in the spectral data in the HNH symmetric bend region. The blue shift suggests that TMAO directly interacts with urea because the shift is not seen in the individual Raman spectra of TMAO or urea in solution. [29]

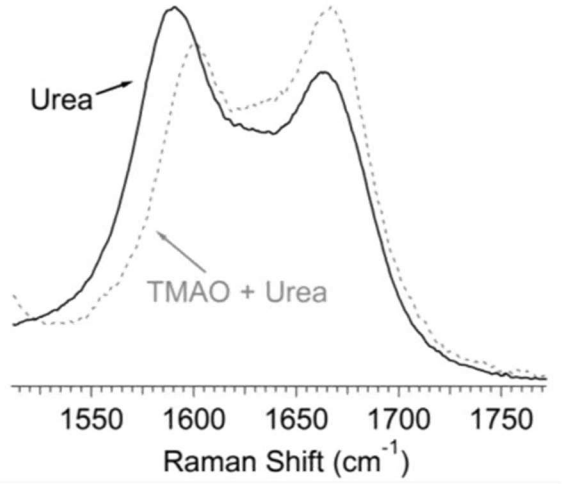

Figure 1.4.2: Blue shift of TMAO and urea solution[29]

1.5 Spectroscopy

The most basic definition of spectroscopy is the study of light matter interactions. Light can be described as either discrete or continuous. Matter can be in the elemental form or as a bonded molecule. The interactions between light and matter ranges from emission, absorption, transmission, scattering and reflection.

1.5.1 Electromagnetic Radiation

Electromagnetic radiation or light refers to the waves of the EM spectrum that carry little pockets of EM energy. The EM radiation is known to exhibit a wave-particle duality meaning that it has properties of both a wave and a particle simultaneously. In most cases light is described and studied as a wave. One can study many different aspects of a wave

including its amplitude, wavelength, and frequency. **Equation 1.5.1.1** relates the wave-like properties of EM radiation.

$$c = \lambda v \qquad \textbf{Equation 1.5.1.1}$$

The above equation shows that wavelength and frequency are inversely related to one another and the constant that relates the two is the speed of light in a vacuum. **Figure 1.5.1.1** is a visual representation of **Equation 1.5.1.2**. The wavelength starts small in the range of femtometers with γ-rays and increases in wavelength to gigameters with radio waves. The frequency has the opposite relation by starting with low frequency with radio waves and increases to high frequency with γ-rays. Our eyes are only capable of detecting light in the visible spectrum that only makes up a minute fraction of the entire EM spectrum. The particle-like property of light can be described using **Equation 1.5.1.2**

$$E = hv \qquad \textbf{Equation 1.5.1.2}$$

Light in the particle sense carries with it a packet of energy described as a photon. A photon of energy is described in terms of the frequency. The energy and frequency are directly related with the constant term being Planck's constant. On the EM spectrum, γ-rays would contain the highest energy whereas radio waves would contain the lowest amount of energy. The two equations above both contain the variable frequency allowing for the two equation to be combined into one, **Equation 1.5.1.3** [30]

$$E = \frac{hc}{\lambda} \qquad \textbf{Equation 1.5.1.3}$$

There are many different types of spectroscopy to choose from when studying the effects of light on matter. The different sections of the EM spectrum will help in studying different aspects matter. A key aspect to look out for is that each type of spectroscopy has requirements that must be met to use it as a viable technique. For example, when using IR spectroscopy, the molecule moiety studies must have a net change in dipole moment. An in-depth look at Raman spectroscopy will be discusses later.

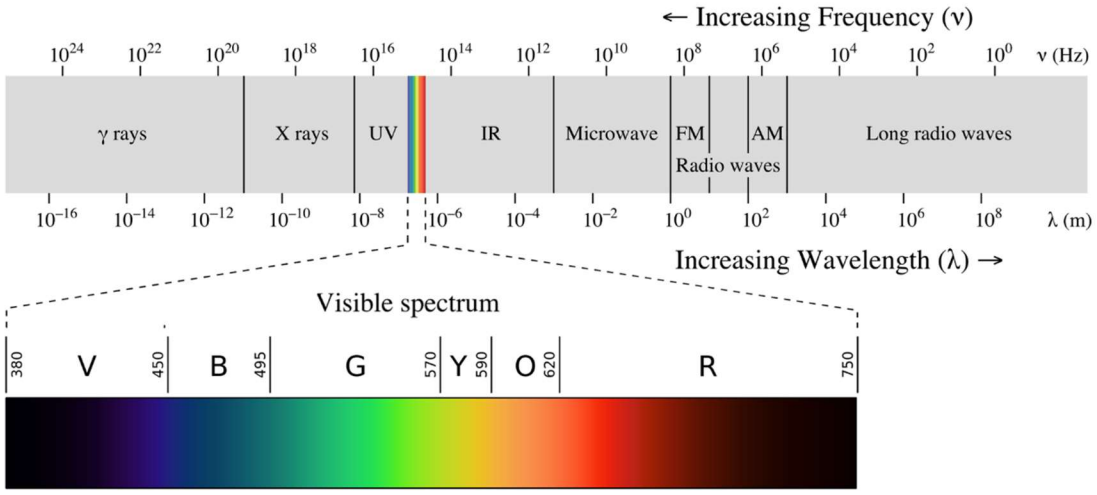

Figure 1.5.1.1 Electromagnetic spectrum [31]

1.5.2 Transitions

All forms of matter; atoms, ions, and molecules, are in constant motion all the time. The type of movement can be dependent on the form of matter being studied. Molecules have four types of transitions that occur to them: translational, rotational, vibrational, and electronic. A visual representation of the various types of movement can be seen in **Figure 1.5.2.1**. Translational movements involve the entire molecule moving in unison in a three-dimensional plane. Translational transitions require the least amount of energy to occur. A rotational transition involves an axis of rotation that usually dissects a central atom. The

rest of the atoms are spun around this axis of rotation. A rotational transition occurs when EM radiation from a microwave source is directed towards a molecule. The molecule must contain a permanent dipole moment to absorb the microwave energy and induce a rotational transition. The next highest energy transition is a vibrational transition that consist of two types of movements: bending and stretching. The stretching may be symmetric meaning that the movement is of the same magnitude on either side or asymmetric where the movement is not uniform. A vibrational excitation occurs with a light source from the infrared region of the EM spectrum. A molecule must have a nonzero dynamic dipole moment to elicit a vibrational excitation to occur. The final and highest energy transition is an electronic transition. Electronic transitions are a result of the excitation of visible and ultraviolet radiation. Some electronic transitions can be detected without the need for specialized instrumentation. A color change that occurs in the visible region of the EM spectrum is a direct indicator that an electronic transition has occurred with the sample being observed. [32]

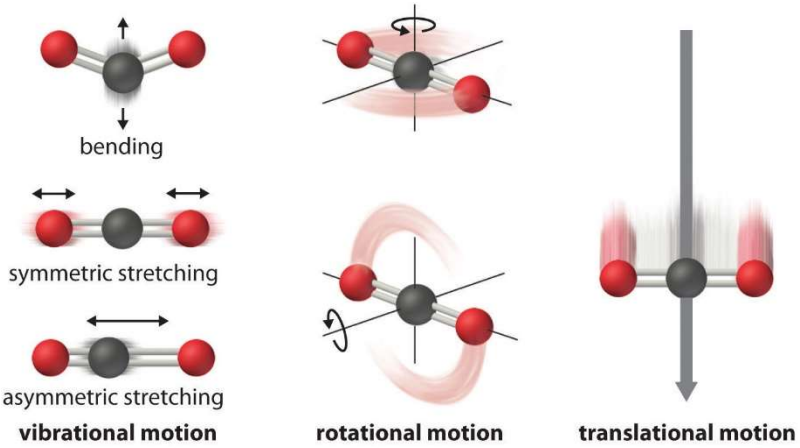

Figure 1.5.2.1 Types of molecular motion [33]

From the hierarchy stated above in respect to transitions, one can create a graph where there is an electron level that contains multiple vibrational transitions within it along

with multiple rotational transitions within the vibrational transitions. **Figure 1.5.2.2** shows how the different transition states are arranged according to energy and nuclear separation. Vibrational transitions can be described using two different systems. With a harmonic oscillator the vibrational levels are equally spaced and the lines on either side are not asymptotic. The other system is the anharmonic approximation where the energy levels decrease as the vibrational level increases and nuclei cannot pass through one another because the graph does not cross the y axis. The rotational levels decrease in distance between levels as the rotational level increases. Rotational states also can go beyond the vibrational state in which the series started. In **Figure 1.5.2.2**, rotational states five and six reach beyond vibrational level one moving into the next vibrational level.

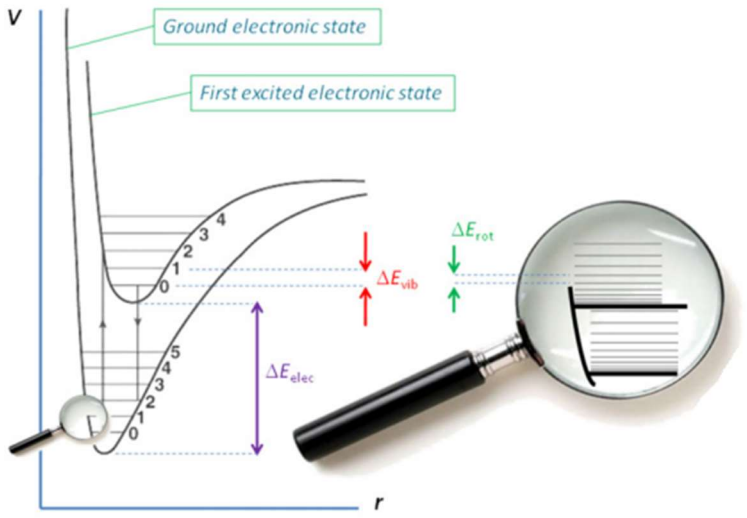

Figure 1.5.2.2 Electronic, vibrational, and rotational states [34]

Selection rules help govern what types of transition are allowed. The vibrational states, often referred to as a harmonic oscillator can have transitions where Δ v=+-1. A fundamental transition occurs when the starting state is v=0. When the starting state is v>0 then the transition is called a hot band. Hot bands are usually only observed at elevated

temperatures. When Δ v>=-1 an overtone is produced. Overtones can be produced because molecules are anharmonic. The rotational states also referred to as a rigid rotor model can have transitions where Δ J=+-1. Rotational transitions consist of three different types or branches. A Q branch occurs when Δ J=0 implying that only a vibrational and/or an electronic transition occurred. The higher energy R branch occurs when the Δ J=+1 whereas the lower energy P branch arises when Δ J=-1. At room temperature it is assumed that the vibrational and electronic states of a molecule will be in the ground state. The above assumption only holds true if the amount of thermal energy available is less than the energy gap between states. The rotational states will however be populated above the ground states of molecules at room temperature. This phenomenon causes spectrum obtained from UV-vis and IR to contain broad peaks. [32, 34]

1.6 Raman Spectroscopy

1.6.1 Introduction

Raman spectroscopy is an analytical vibrational spectroscopy technique that is similar and complementary to IR spectroscopy. Raman is a nondestructive technique that requires little to no sample preparation. Because of newer design and lower cost of manufacturer, Raman spectroscopy is moving out of the research labs and into the private sector along with into the hands of the layperson. [35] Raman spectroscopy is becoming more valuable in the field of forensic chemistry because of its nondestructive nature and ability to analyze a plethora of different compounds. A portable Raman spectrometer has been created and is used to identify illicit drugs. Police and forensic scientist can analyze an unknown substance in the field using a portable Raman and can obtain an accurate analysis of the identity of the unknown substance. [36] Raman spectroscopy has been successfully used to analyze questionable documents for their authenticity by analyzing the

inks from such documents along with the ability to successfully compare fibers from a crime scene to fibers from another source for similarities. [22, 37] The nondestructive nature has been used to differentiate different bodily fluids in a forensic setting. Dry samples of blood, semen, saliva, sweat, and vaginal fluid were differentiated from one another and canine semen was differentiated from human semen all using Raman spectroscopy [38]

1.6.2 Background and Theory

In 1928, Sir C. V. Raman successfully observed the scattering of light that would eventually be known as Raman scattering. Raman created an experiment using his eye as the detection source and determined that there were two different phenomena occurring when a light source was scattering by molecules. One type of scattering resulted in a wavelength that was the exact same wavelength of the light source and the other type of scattering resulted in a wavelength of light different than the source. Along with the variation in wavelengths of the scattered light, Raman also noticed that there was a change in the frequency of the scattered light compared to the source that was characteristic of the molecule being tested. Sir C. V. Raman obtained a Nobel Prize in Physics for his discovery of this phenomenon occurring as a result of scattered light. [35, 39]

As it was mentioned earlier, there are two types of scattering that may occur, Raman and Rayleigh scattering. The predominant form of scattering found in nature is Rayleigh which occurs when the scattered light is of the same wavelength as the original source light. The type of collisions that occur with Rayleigh scattering are called elastic collisions because there is no net change in energy or wavelength from the incident light to the scattered light. An example of this can be seen in spy movies. When the spy goes to steal

some valuable object they usually encounter a room that looks normal until the spy sprays an aerosol or throws a fine powder in the air. After they do this a plethora of various lasers are then able to be seen by the human eye. Before the extra particles are introduced to the room the lasers were not detectable by the human eye because one would have to be staring directly at the laser to be able to see it. The introduction of the particles causes the laser sources to interact with the particles causing the laser light to scatter as a result. The scattered light is predominately Rayleigh scattering because the laser light is of the same color or wavelength as the original laser light.

The less common type of scattering occurring in nature is known as Raman scattering. Raman scattering occurs because of inelastic collisions meaning that there is a net change in energy from the incident light to the scattered light. There are two types of Raman scattering, Stokes and anti-Stokes Raman scattering. Stokes scattering occurs when a photon from the light source loses energy because of interacting with an object. A ground state electron is excited to a virtual energy state and returns to a higher energy level than it started on. In anti-Stokes scattering, a non-ground state electron is again excited to a virtual energy state and returns to a lower energy state than it started with. Anti-Stokes scattering is less common than Stokes scattering because at room temperature most molecule will be in the vibrational ground state. [30, 35, 40] **Figure 1.6.2.1** shows the different types of scattering that may occur along with an example of how IR absorption compares. The color and thickness of the lines are related to the different types of scattering. The color difference shows a change in energy of light and the thickness is a rough estimation of the probability of each type of scattering.

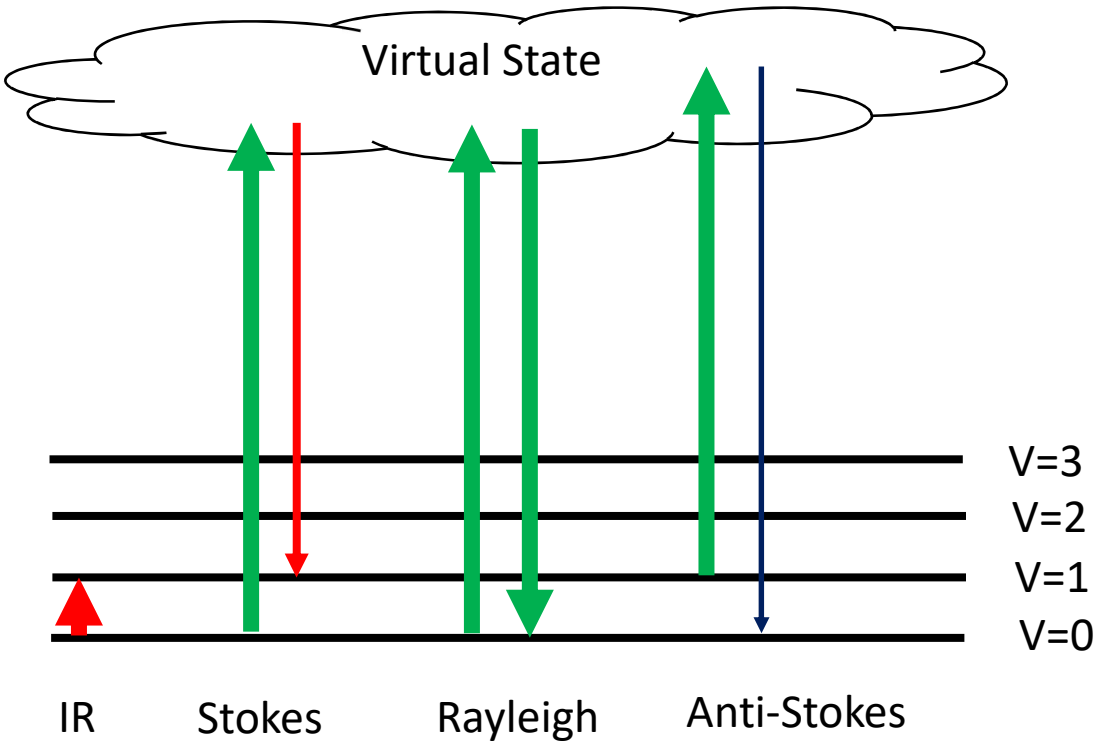

Figure 1.6.2.1: Types of scattering

The energy change in the system can be calculated from **Equation 1.6.1.2** where the change can be calculated using hv. With scattering light, the amount of energy is not quantized like in IR where the absorption of a photon is quantized. Because the scattering of light is not quantized, the energy is not enough to reach the excited states. The molecule is thus said to be in an imaginary state that is called a virtual state. The virtual state represents a place between the excited and ground state that an electron will temporarily occupy. To find the different vibrational energy changes of the molecules **Equation 1.6.2.1** can be used.

$$E - \Delta E = h(v - v_1) \quad \textbf{Equation 1.6.2.1}$$

The above equation is used to obtain the various shifts in frequency from the Rayleigh frequency. Wavelength is not present in the equation making the wavelength of

the laser or excitation source independent of the frequency shifts. In theory the same Raman data can be obtained using an excitation source that is in the visible, IR, or UV region of the EM spectrum. [40]

The graphical representation of Raman spectroscopy is like that of IR spectroscopy. Like IR, Raman is also plotted as intensity versus the shift in wavenumber. The intensity is arbitrary and is depicted as the number of times that a signal at that wavelength returned to the detector. The units for intensity are usually depicted as Raman intensity and the numerical values are often left off the y-axis. The x-axis, on the other hand, is in the units of wavenumber and labeled as Raman shift. Since the units are in wavenumbers, the Raman spectrum can easily be compared to the IR spectrum because the Raman shift in wavenumbers is identical to the absorption peak in wavenumbers from IR. A key difference between the two analytical techniques is what kinds of molecules can be studied in each one. In IR spectroscopy the molecules must possess a change in dipole moment. A molecule must have a change in polarizability to be Raman active. If a vibrational mode is both IR and Raman active a peak will appear in the exact same place in both spectrum. There may, however be a difference in the intensity of the two peaks. The Raman spectrum are usually of a lower intensity because the probability of Raman scattering is much lower than that of Rayleigh scattering and IR absorption A conventional difference between IR and Raman is that the IR graph are usually depicted as the peaks going down or in the negative whereas the Raman peaks are pointed up and positive.

1.6.3 Raman Light Source

A Raman spectrometer has a few basic pieces to function properly: a sample holder, light source, wavelength selector, and a detector. The light sources required for Raman

spectroscopy must be monochromatic. The power of the light source is directly proportional to the resulting Raman signal. The original light sources were made from a UV light source that was weak making the resulting Raman signals small or non-detectable. Today, a more powerful laser light source is used to increase the signal-to-noise ratio along with the intensity of the Raman scattering. Lower wavelength light sources create more intense signals than higher wavelength sources because Raman scattering is proportional to the light source frequency by **Equation 1.6.3.1**. The disadvantage to using lower wavelength light sources like blue and green is that they may cause a sample to decompose or fluoresce. The longer wavelength light sources are thus preferred for material that may fluoresce like some biological material. When choosing the excitation source for your sample it is imperative that your sample does not absorb at the same wavelength as the excitation source. [30]

$$\frac{1}{\lambda^4} \qquad \textbf{Equation 1.6.3.1}$$

1.6.4 Temperature Control Stage

A THMS600 heating and freezing stage that has a temperature range of -196 to 600℃ was used to obtain spectra at low temperatures. The stage was accompanied by a T95 LinkPad, LNP95 cooling pump, and a 2L Dewar. **Figure 1.6.4.1** shows how the TCS is set up on the Raman spectrometer. The following set up allows the user to take Raman spectrum of their sample at both high and low temperatures. For this experiment the focus will be on using the TCS for taking Raman at low temperatures. To use the low temperature setting on the TCS, liquid nitrogen is needed. Liquid nitrogen has a boiling point at -196℃ or 77 Kelvin allowing the user to cool their samples down to that temperature.

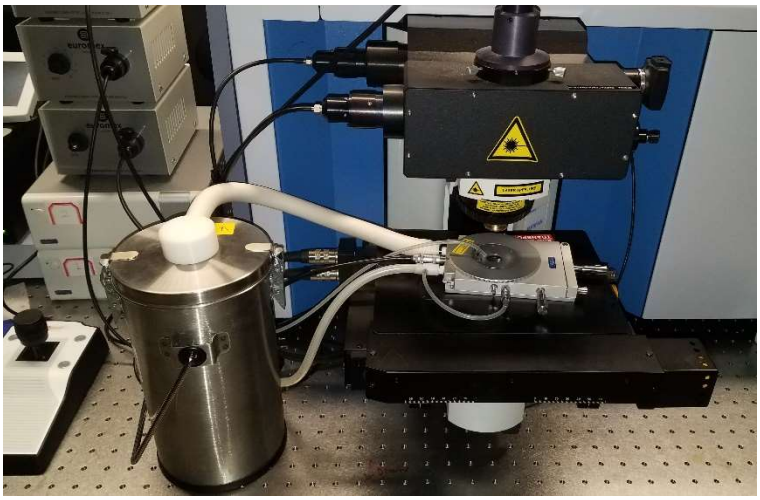

Figure 1.6.4.1: Photograph of TCS setup

Chapter 2: Experimental

2.1 Instrumentation

The primary instrumentation used for the data of this research was a Horiba HR Evolution Raman Spectrometer. The excitation sources used to obtain spectra was a YAG 532nm laser. The green 532nm laser was used because it is the most powerful laser that was available and none of the samples tested absorbed light at 532nm allowing for optimal scattering.

The Raman spectrometer was calibrated before any spectra were taken on it each day. The process for calibrating the Raman was simple and usually took less than five minutes. The green 532nm laser was first turned on. Then a calibration slide containing a sample of a silicon wafer is placed under the aperture of the Raman. **Figure 2.1.1** shows a visual of what the stage and apertures on the Raman spectrometer look like. A 10x objective lens was used in all cases to obtain the spectra. A CCD camera was used to find the sample on the slide. A joystick was used for fine movements to obtain a clear image of the silicon wafer. Once the silicon wafer was found on the calibration slide using crosshairs on the screen, the Raman was then ready to calibrate. Auto calibrate was hit using the parameters of a 532nm laser and 600gr/mm grating. The calibration of the Raman results in finding the zero point along with the vibrational peak associated with the silicon wafer at approximately 520cm^{-1}. Once these two peaks were found, the instrument was then calibrated to the above settings and ready to collect data.

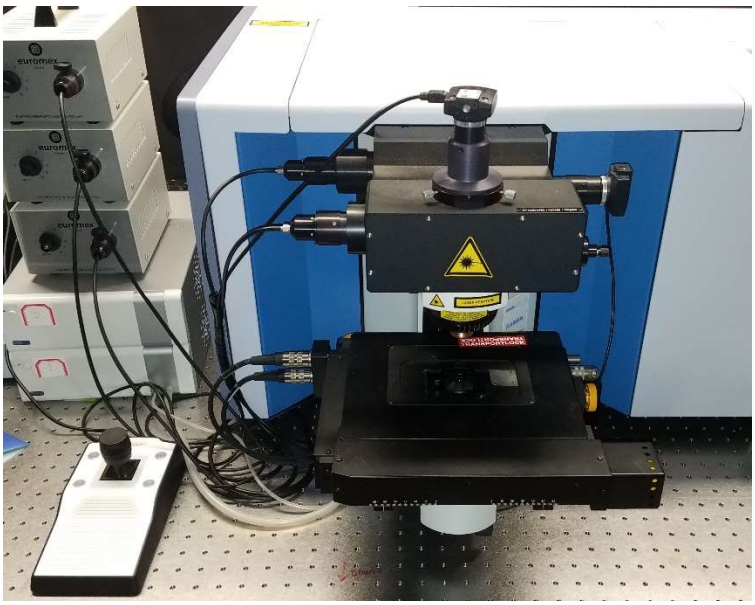

Figure 2.1.1: Photograph of Raman stage

2.2 Sample Preparation

One of the best attributes with using Raman spectroscopy is the little to no sample preparation needed to take data. All the data was taken from various iteration of three different osmolytes: urea, gdn-HCl, and TMAO. **Tables 2.2.1**, **2.2.2** and **2.2.3** show the different solutions and samples that were created and tested. Each of the solutions were made by adding DI water to the solid osmolyte. All the solid osmolyte added to each solution dissolved completely making each solution colorless with no visible undissolved osmolyte present. The osmolytes were all supplied by Sigma-Aldrich and were not purified any further. The purifications were as followed: urea $\geq$ 98.0%, gdn-HCl $\geq$ 98.0%, and TMAO $\geq$ 99.0%.

Table 2.2.1: Serial dilutions

1M Urea	2M Urea	4M Urea	6M Urea	8M Urea	Solid Urea
1M Gdn-HCl	2M Gdn-HCl	4M Gdn-HCl	6M Gdn-HCl	8M Gdn-HCl	Solid Gdn-HCl
1M TMAO	2M TMAO	4M TMAO	6M TMAO	8M TMAO	Solid TMAO

Table 2.2.2: Osmolyte solutions

1 Urea: 1 Gdn-HCl	1 Urea: 2 Gdn-HCl	2 Urea: 1 Gdn-HCl
1 Urea:1 Gdn-HCl	1 Urea: 1 TMAO	1 Gdn-HCl: 1 TMAO
1 Urea: 1 Gdn-HCl: 1 TMAO	DI Water	

Table 2.2.3: TCS solutions at -150°C

8M Urea	8M Gdn-HCl	8M TMAO
1 Urea:1 Gdn-HCl	1 Urea: 1 TMAO	1 Gdn-HCl: 1 TMAO
1 Urea: 1 Gdn-HCl: 1 TMAO	DI Water	

2.3 Data Collection

Data were only collected from solids and liquids for the experiment. The solid samples were placed on a microscope slide. A small amount of sample, the size of a pencil tip, was required to acquire the Raman spectrum of the solids. The CCD camera was used to bring the solid into focus allowing for the user to place the laser on a piece of the solid sample. **Figures 1.2.1.1.1, 1.2.2.1.1**, and **1.2.3.2.1** are all examples of the solid osmolyte samples that the laser had to focus on top of. The final Raman spectra of each sample case was collected using the following settings: an acquisition time of 15 seconds, 15 accumulations, 600 gr/mm grating, and a 100% laser intensity

The microscope slides were unable to be used to sample the various solutions that were created. Instead, a special adapter to the Raman spectrometer was used allowing for solutions to be tested. The attachment shown in **Figure 2.3.1** attaches to the aperture nosepiece or turret by the two screws on either side. Cuvettes were then placed into the holder and tightened using the two white screws on either side. Special cuvettes that had

sloped sides were used to reduce the amount of solution needed to collect data. If sample size was still a problem, the user can adjust the cuvette height using the set screws. The user may temporarily collect real-time acquisitions in a region where there should be a peak to move the cuvette up or down optimizing the perfect placement to collect the best data possible. Once the optimal position was found, the set screws were tightened securing the cuvette in position. When collecting data for liquids, finding the sample using the CCD camera was not required because the sample is already positioned so that the laser must contact it.

Figure 2.3.1: Photograph of Raman spectrometer cuvette holder

The last way that data were collected was using a TCS attached to the Raman spectrometer. The samples found in **Table 2.2.3** are the only ones where the Raman spectra were taken using TCS. **Figure 1.6.4.1** shows what the TCS looks like along with how it is attached to the liquid nitrogen vessel and pumps. A small aliquot of sample, approximately 25 μL, was placed on one end of microscope slide. The sample had to be placed on one end of the microscope slide because of the way the slide sits in the TCS. Once the sample was placed on the slide, the slide was pushed into the TCS and the TCS was sealed. Liquid nitrogen was then carefully poured into the liquid nitrogen vessel approximately three fourths of the way to the top. The TCS was placed on the Raman stage and the viewing

window was aligned underneath the 10x objective lens. The pump was turned on and set to -150℃ with a pump speed of 95. When the temperature reached the desired ending temperature, the pump speed was decreased to negate the system from having to heat the stage which wastes the liquid nitrogen. After the sample crystallized, the CCD camera was used to find the crystals and Raman data were then collected. If the CCD camera was turned on for the freezing of the sample, the formation of the ice crystals were visible along with how the solution moved as crystals formed.

Chapter 3: Data Analysis

3.1 Solid Phase

Solid samples of gdn-HCl, urea, and TMAO were all collected and compared to theoretical data. The theoretical data were calculated using a hybrid density functional Becke 3-parameter Lee-Yang-Parr (B3LYP). The basis set that accompanied the functional was 6-31++G which was used in previous research[41]. The theoretical calculations were carried out using Gaussian 09 software. **Figures 3.1.1, 3.1.2,** and **3.1.3** show a comparison of solid experimental Raman spectra compared to its theoretical counterpart. Gdn-HCl and TMAO showed high correlation between experiment and theory whereas urea had many differences.

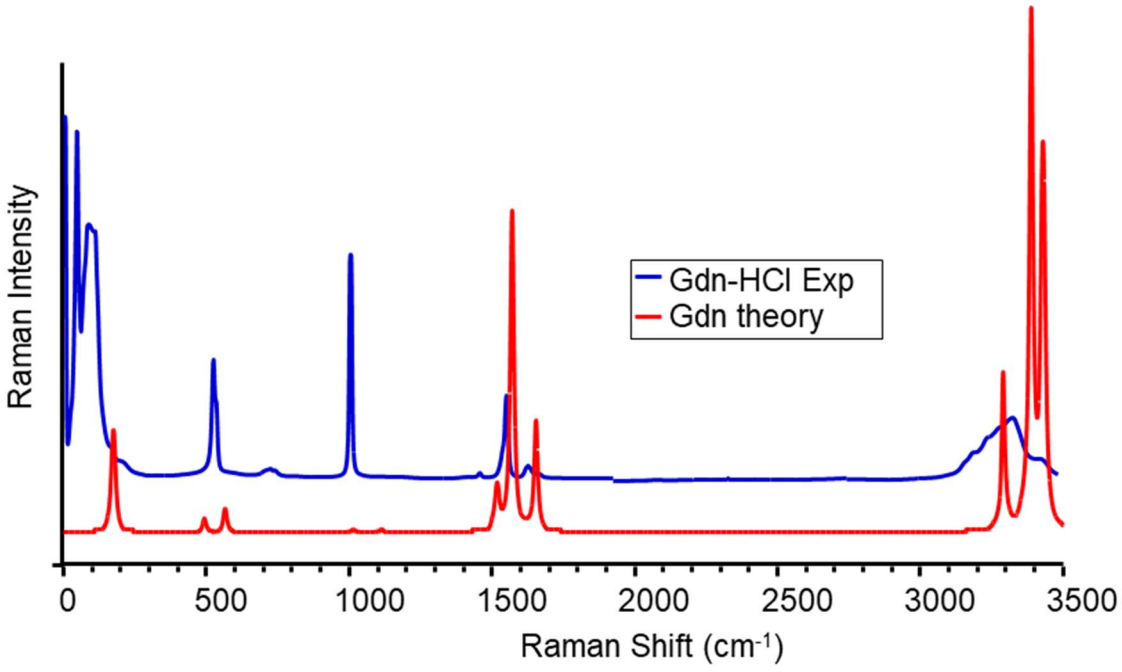

Figure 3.1.1: Raman spectrum solid gdn-HCl experimental versus theory

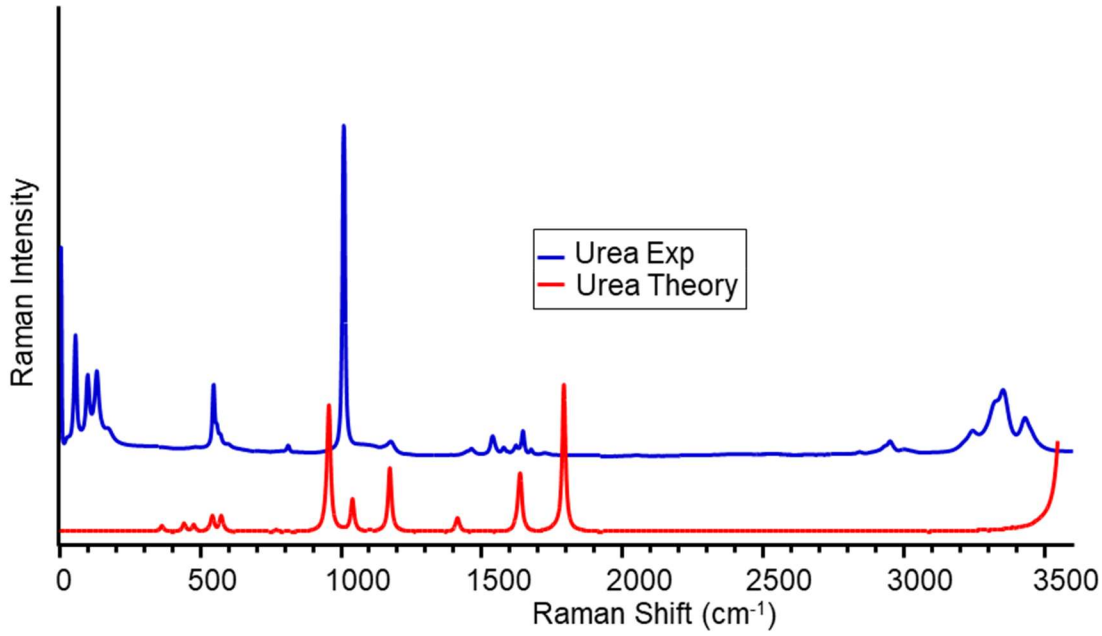

Figure 3.1.2: Raman spectrum solid urea experimental versus theory

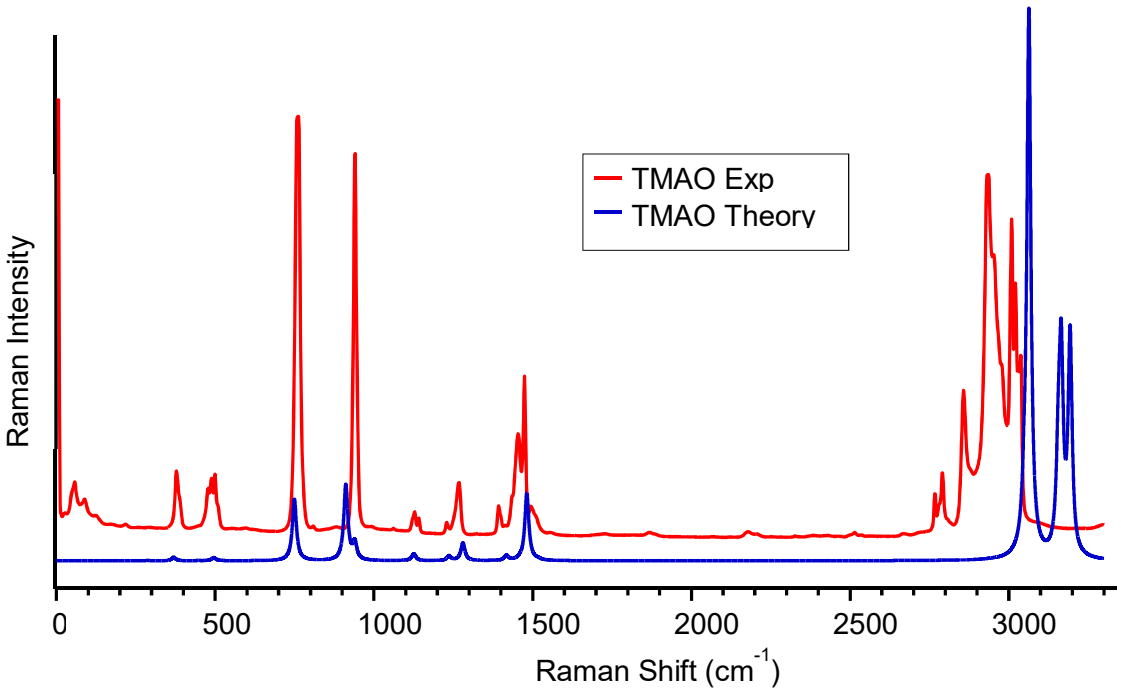

Figure 3.1.3: TMAO experimental versus theory Raman spectra

3.2 Osmolyte Solutions

Data from the serial dilution were collected using the Raman spectrometer and can be seen in **Figures 3.2.1**, **3.2.2**, and **3.2.3**. In each of the graphs there were little deviations in the spectra from one concentration to the next. The small shifts from the samples in solution were of both higher energy (blue) and lower energy (red) compared to the solid sample. The shifts in Raman peaks are consistent with the various osmolytes interacting with water directly. The shifts are also consistent with previous research showing how these osmolytes interact with water.[27, 42] The same peaks were able to be distinguishable on each of the three graphs. It is important to note that there was no manipulation of the intensities allowing all the different spectra to be on the same scale. Each of the spectra was separated from one another to allow for easier identification and were placed in increasing concentration order. The biggest difference found is that the intensities of the various peaks were dependent upon the concentration of the solute.

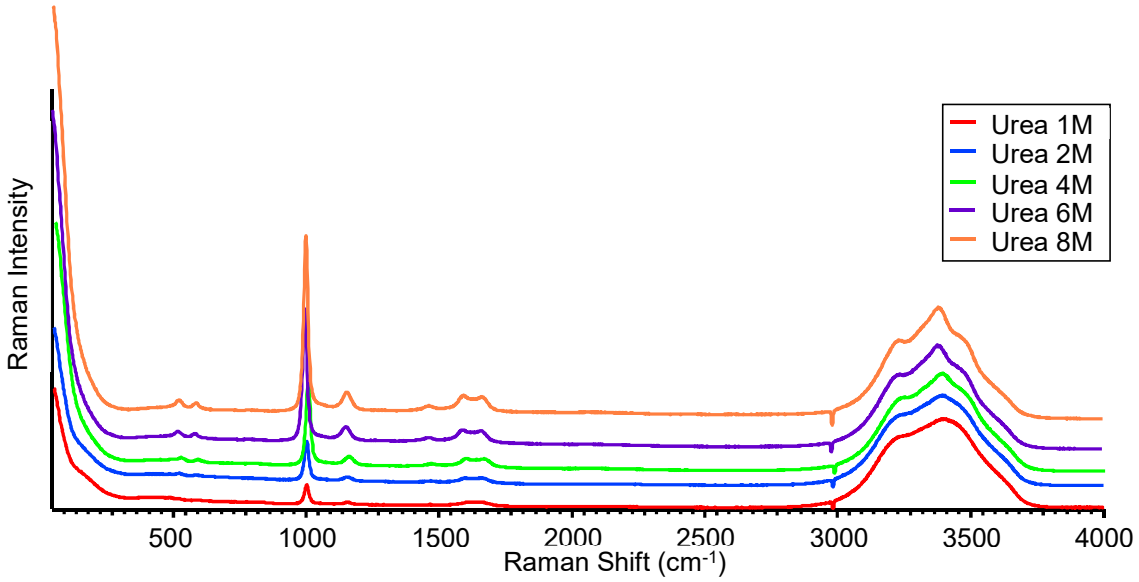

Figure 3.2.1: Serial dilution of urea

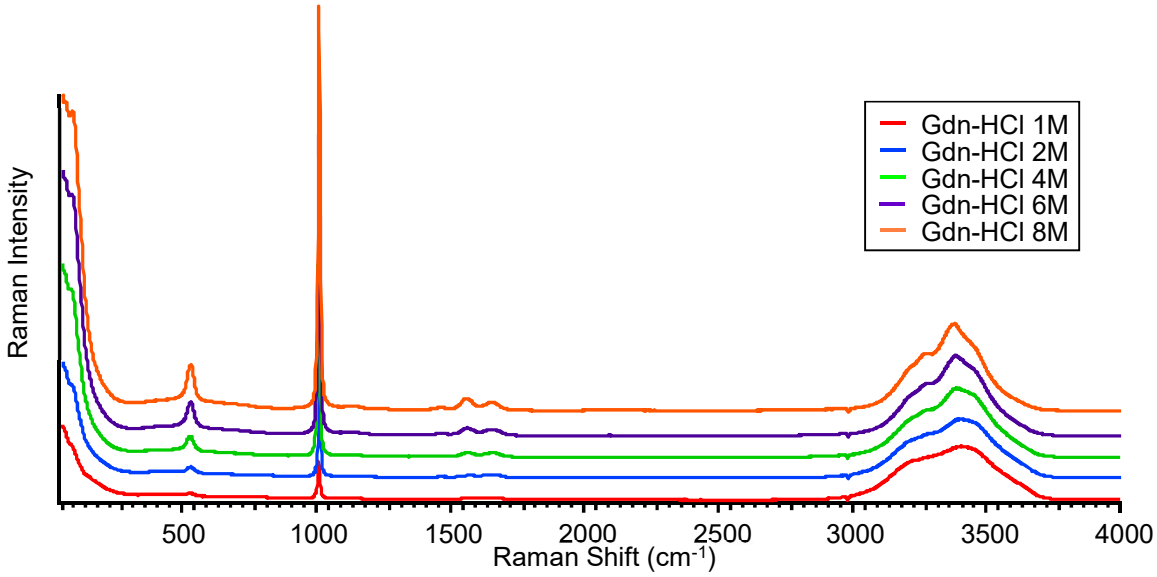

Figure 3.2.2: Serial dilution of guanidine hydrochloride

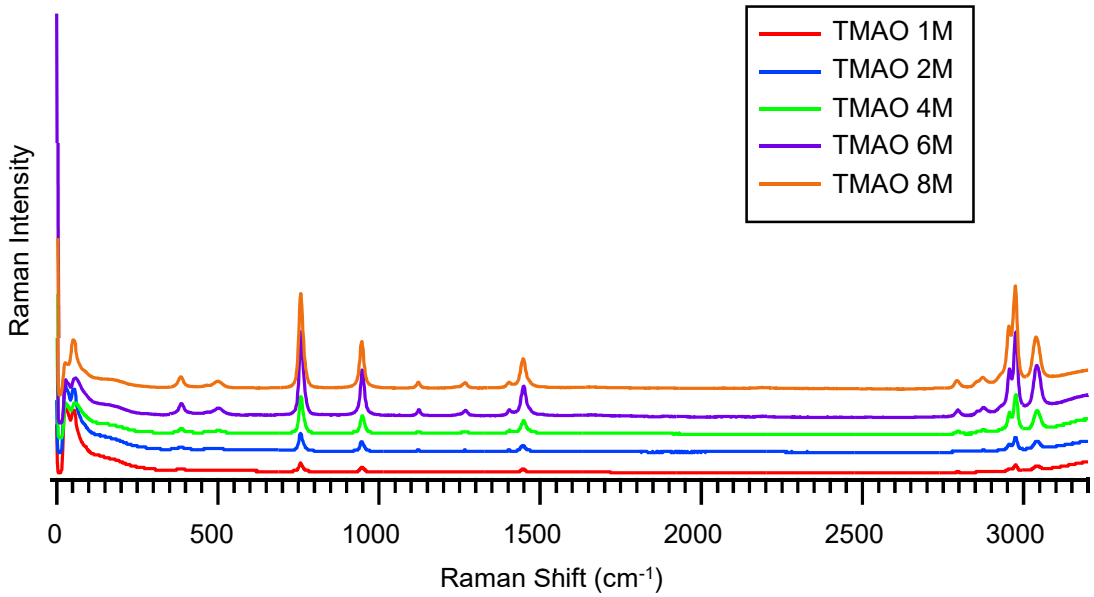

Figure 3.2.3: Serial dilution of TMAO

3.3 Osmolyte Interactions

The first part of this section will look at confirming previous research conclusions using new data. The interaction of urea and TMAO have already been studied by the Hammer research group and it was concluded that TMAO interacts directly with urea causing a blue shift in a peak at 1591cm^{-1}. That peak was found to be associated with the HNH bend found in urea. The spectrum collected in **Figure 3.3.1** is consistent with previous research. A concentrated view of the important region around 1600cm^{-1} can be seen in **Figure 3.3.2.** The blue shift observed in **Figure 3.3.2** is consistent with previous research that can be seen in **Figure 1.4.2**. There was a small difference in the degree of shift from previous research to current research. Previous research showed an 11cm^{-1} blue shift whereas **Figure** 3.3.2 exhibits a 6cm^{-1} blue shift.

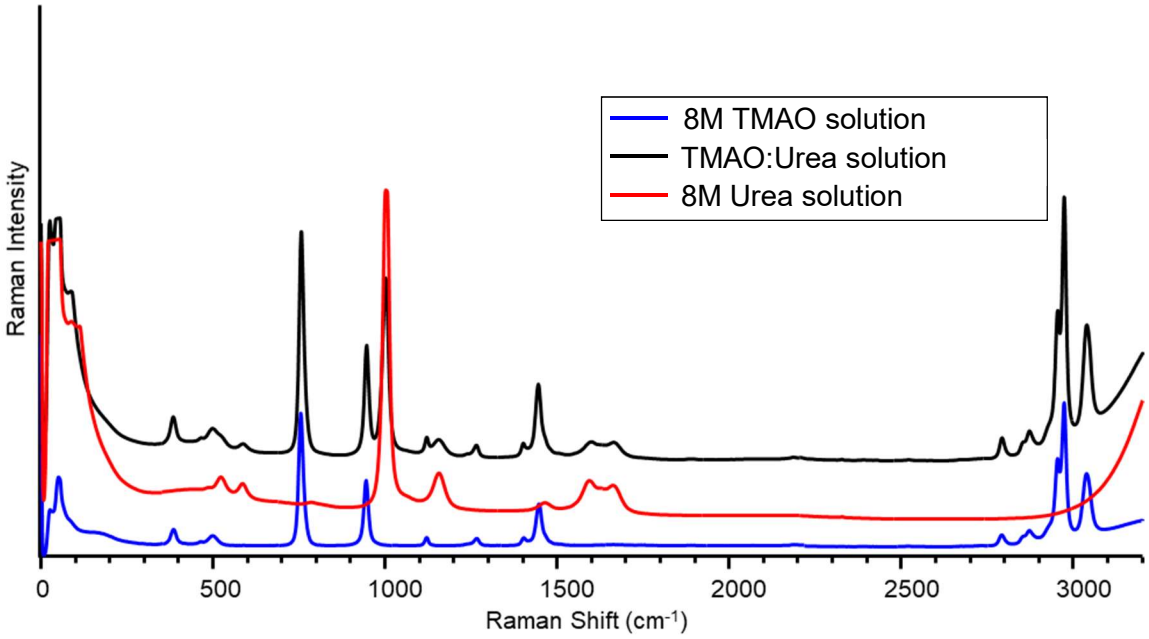

Figure 3.3.1: Raman comparison of solutions involving TMAO and urea

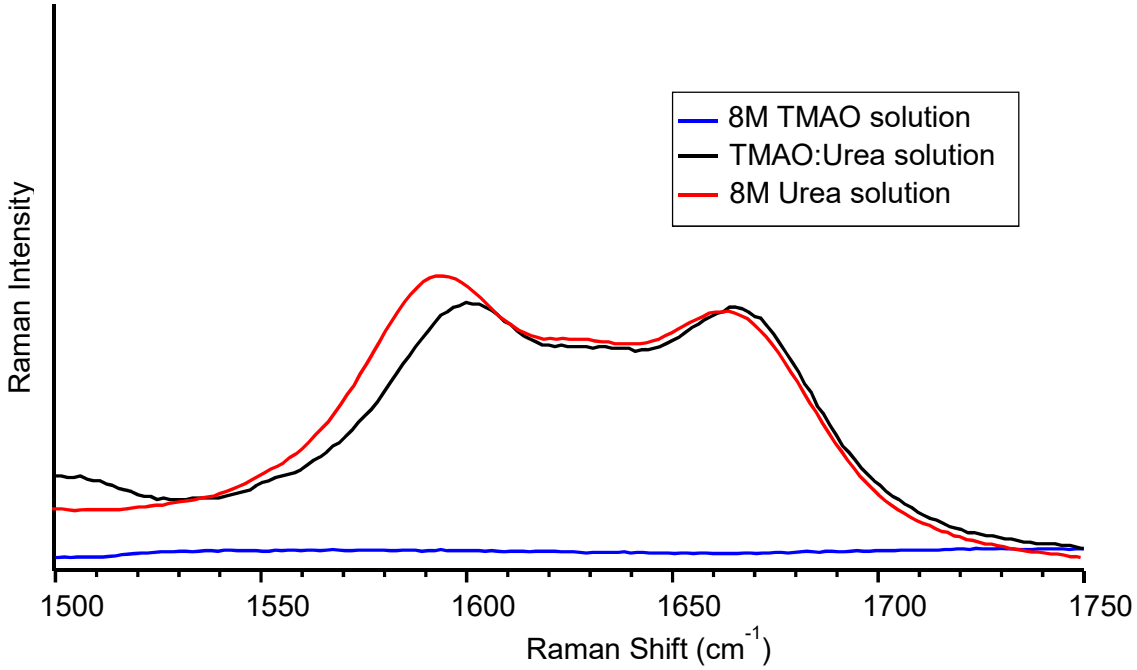

Figure 3.3.2: Raman comparison of solutions involving TMAO and urea at HNH bending region

The new aspect of the research aims to study the interaction between TMAO:gdn-HCl and the interactions of urea:gdn-HCl. The Raman spectrum for gdn-HCl is like that of urea with only a few differences and can be seen in **Figure 3.3.3**. In the urea spectrum there are two peaks at 524cm^{-1} and 587cm^{-1} whereas gdn-HCl only has one peak at 529cm^{-1}. Another area of difference occurs in the HNH bending region. Urea has a peak at 1594cm^{-1} whereas gdn-HCl has that same peak at 1556cm^{-1}. When the two solutions are combined there are a few changes in the spectrum compared to each individual solution. In the 1:1 ratio solution there is a single peak at 530cm^{-1}. The resulting singular peak could be additive from the two peaks in urea with the one peak of gdn-HCl. The spectral range between 1500-1800cm^{-1} is of the most importance because it contains the HNH bending region. When urea and gdn-HCl are combined the resulting peak occurs at 1598cm^{-1}. The related peak in the urea spectrum is at 1595cm^{-1} and at 1558cm^{-1}. In both cases a blue shift could be associated with the resulting solution of the two osmolytes; however, one can't confirm a shift occurred because each individual osmolyte contains a peak in the region. The resulting peak could be the summation of the two individual osmolytes.

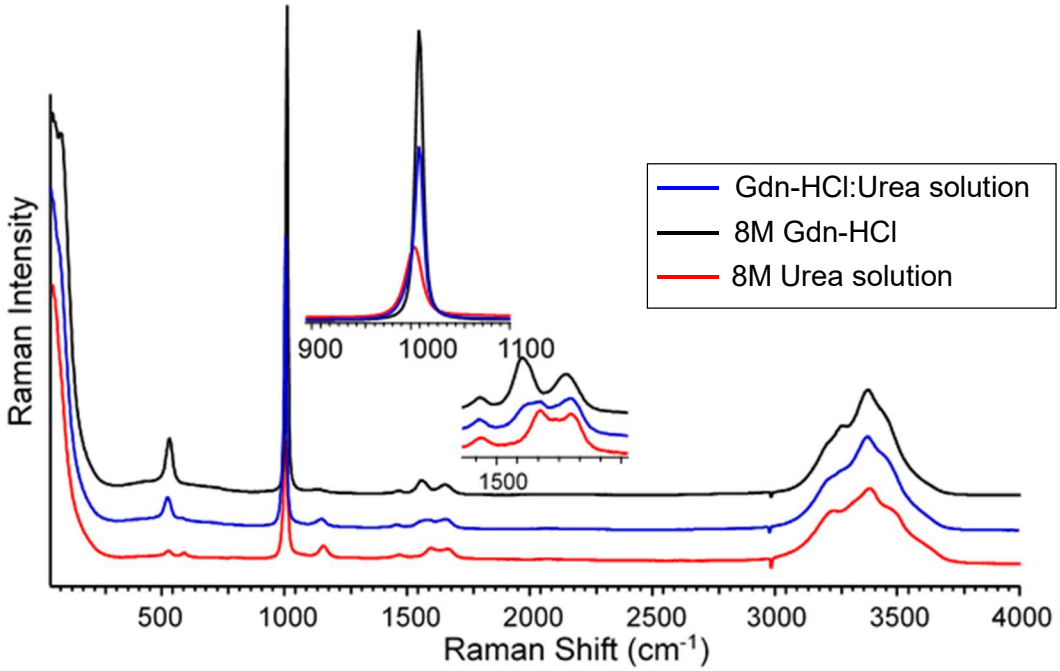

Figure 3.3.3: Raman comparison of solutions involving gdn-HCl and urea

The next part of the research focused on the interaction of TMAO with gdn-HCl. **Figure 3.3.4** is the resulting Raman data that was taken with the different spectrum separated to make it easier to analyze. The black spectrum is the combination of the two solutions and can be seen to be a combination of the two individual spectra. The two peaks around 500cm^{-1} in both the TMAO solution and gdn-HCl solution can be seen to combine in an additive nature into one broader peak in the black spectrum. Unlike the solution containing gdn-HCl and urea, the solution with TMAO and gdn-HCl do not contain similar peaks in the HNH range of interest. The HNH bending region can be seen up close in **Figure 3.3.5**. The figure shows that there are two peaks where a shift occurs. A shift is confirmed because the spectrum of TMAO has no peaks in the region of interesting causing the only reason for shifting is that interaction of TMAO with gdn-HCl. The first peak shifts to a higher energy (blue shift) going from 1556cm^{-1} to 1566cm^{-1} making a total change of

10cm^{-1}. The second peak also shifts to a higher energy (blue shift) from 1650cm^{-1} to 1660cm^{-1} making the total change in energy of 10cm^{-1}. The two peaks that showed an increase in energy were both associated with bending frequencies of the HNH bond. The peaks associated with TMAO were not found to show any shifts when added to gdn-HCl.

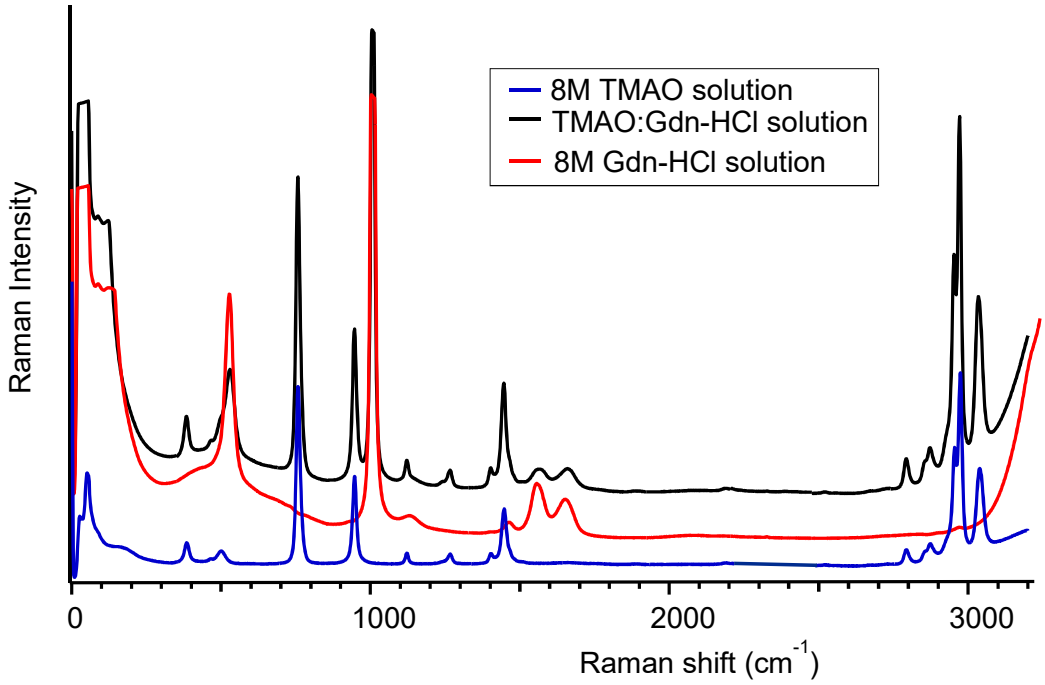

Figure 3.3.4: Raman comparison of solutions involving gdn-HCl and TMAO

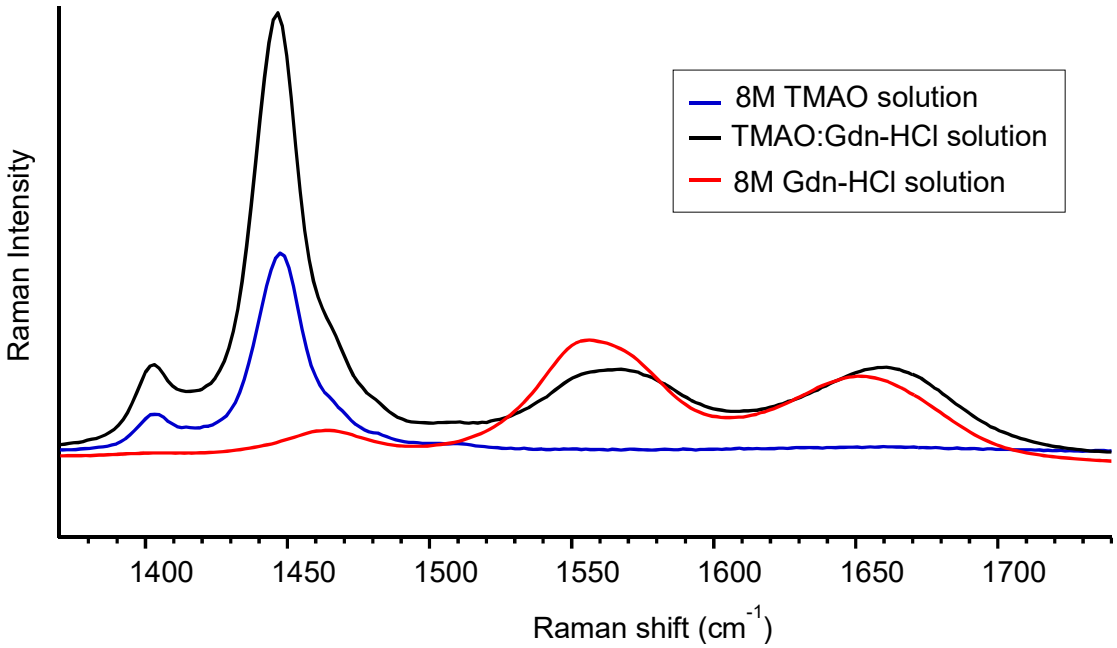

Figure 3.3.5: Raman comparison of solutions involving gdn-HCl and TMAO in the HNH bending region

The three different osmolytes have been studied separately thus far by only comparing solutions made from two of the osmolytes. The next topic was to see what would happen if a solution was made using urea, gdn-HCl, and TMAO. The resulting spectra can be seen in **Figure 3.3.6**. The initial analysis is that there is no observable change or significant shift in vibrational peaks from the individual solutions. The shifts that have been seen thus far are due to the interaction of TMAO with either of the two denaturants. **Figure 3.6.7** is a graph comparing a solution of urea and gdn-HCl with a solution of TMAO, urea, and gdn-HCl in the HNH bending region. It appears that the solution containing TMAO does not show any shifts in the spectrum like it did in individual solutions of TMAO and a denaturant. No shifts may suggest that there are no direct interactions between TMAO and the two denaturants in solution. That result contradicts previous research that showed a shift in the Raman spectra when TMAO was added to both urea and gdn-HCl separately.

These results could be justified by the concentration of the solutions that were used. An equal amount of 8M of each osmolyte was combined into a single sample. The concentration of TMAO was half that of the total concentration of denaturant which could have caused too low of interaction to detect with the Raman spectrometer.

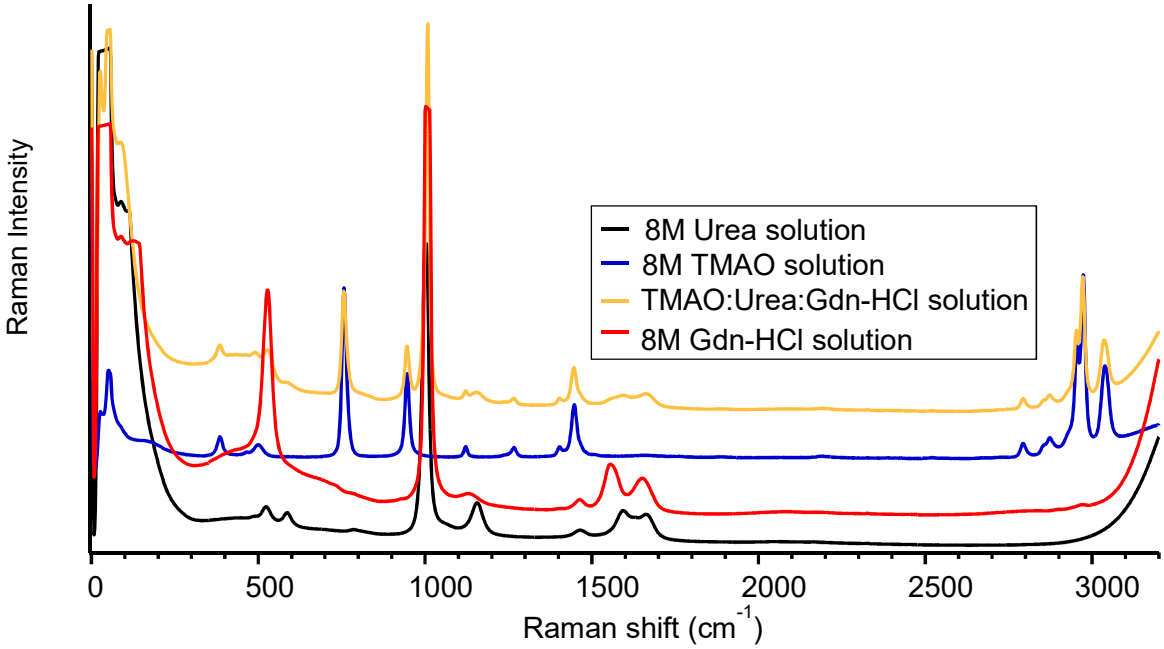

Figure 3.3.6: Raman comparison of solutions involving gdn-HCl, urea, TMAO, and a solution of all three osmolytes

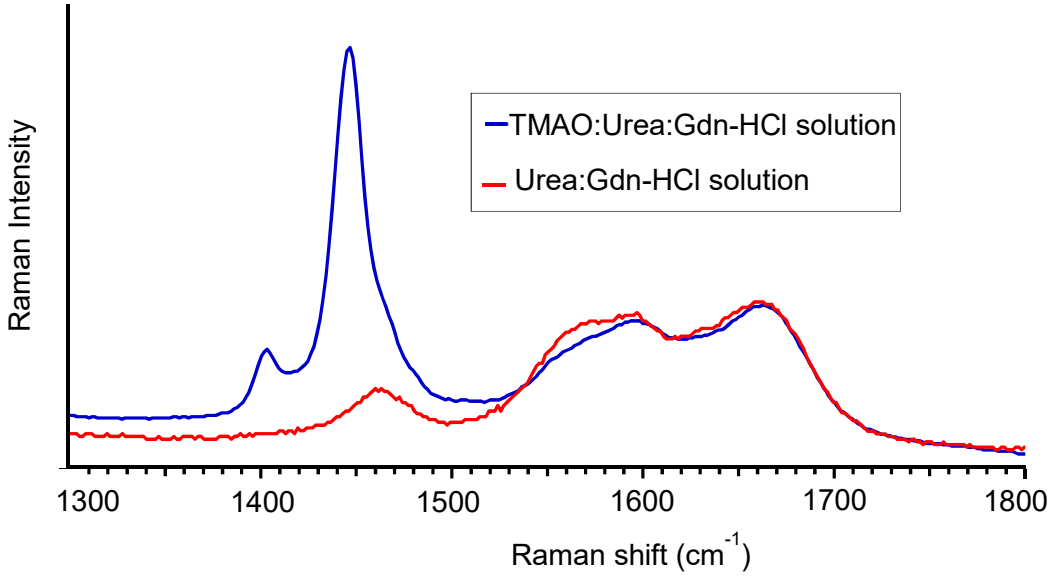

Figure 3.3.7: Raman comparison of solutions involving gdn-HCl:urea and gdn-HCl:urea:TMAO at the HNH bending region

3.4 Temperature Control Stage Analysis

The temperature control stage was used to collect data at temperatures around -150℃ for the entire duration of the Raman scan. The resulting spectra can be seen compared to their room temperature counterparts in **Figures 3.4.1, 3.4.2, 3.4.3**. The spectrum at low temperature for urea was the only that showed a significant amount of deviation from the room temperature counterpart. The low temperature spectrum separated the broad peaks in the HNH bending region in urea and can be seen in **Figure 3.4.1**. A downside to collecting Raman at low temperatures is the Raman intensity decreases greatly. The low temperatures cause the probability of an electron to excite into the virtual state to decrease. When the graphs are normalized, the spectra of low temperatures Raman are seen to have a low signal to noise ratio and the spectrum appears jagged. The low

temperature also causes the solutions to freeze inside the temperature control vessel. The action of freezing the solution in a rapid manner causes the bonds to become more rigid, locking them into place compared to the room temperature solution. That could cause the molecules to be frozen in an unnatural conformation causing the vibrational frequencies to be altered.

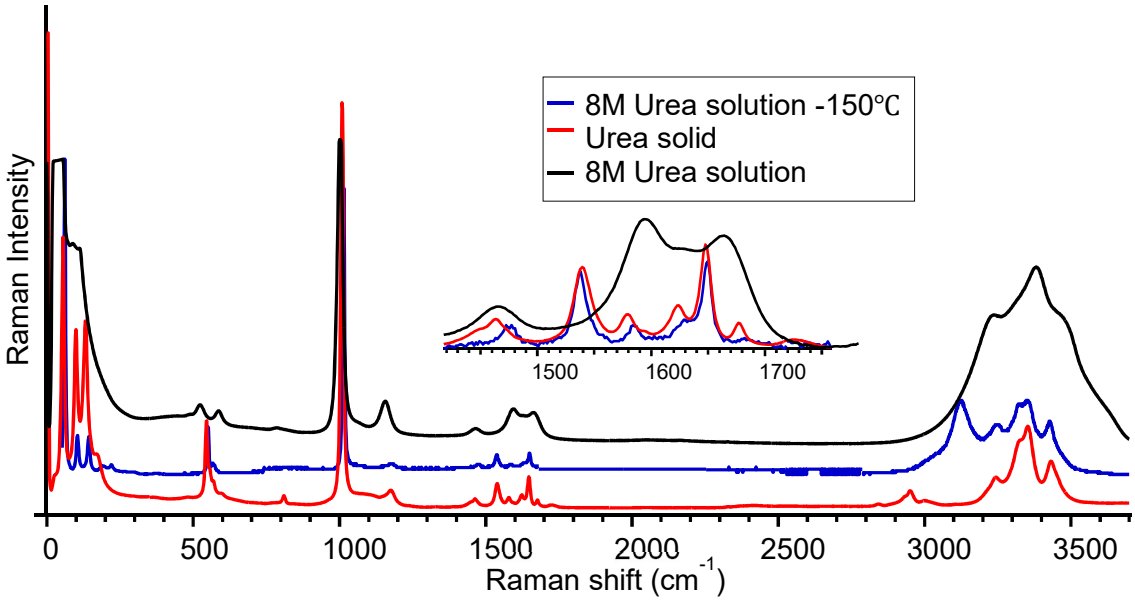

Figure 3.4.1: Raman spectral comparison of urea using temperature-controlled Raman

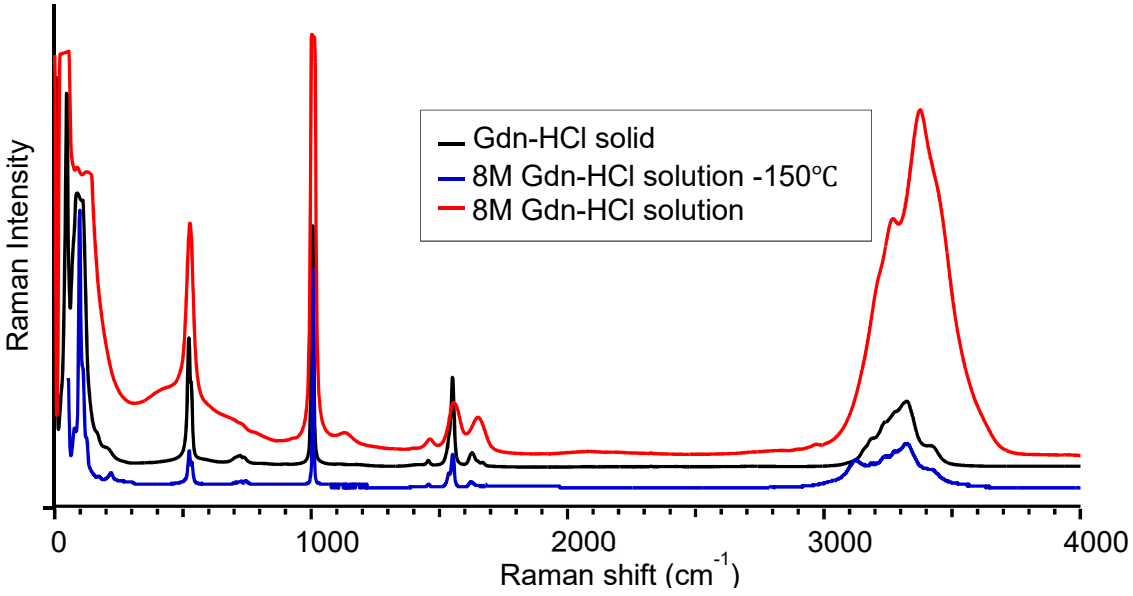

Figure 3.4.2: Raman spectral comparison of gdn-HCl using temperature-controlled Raman

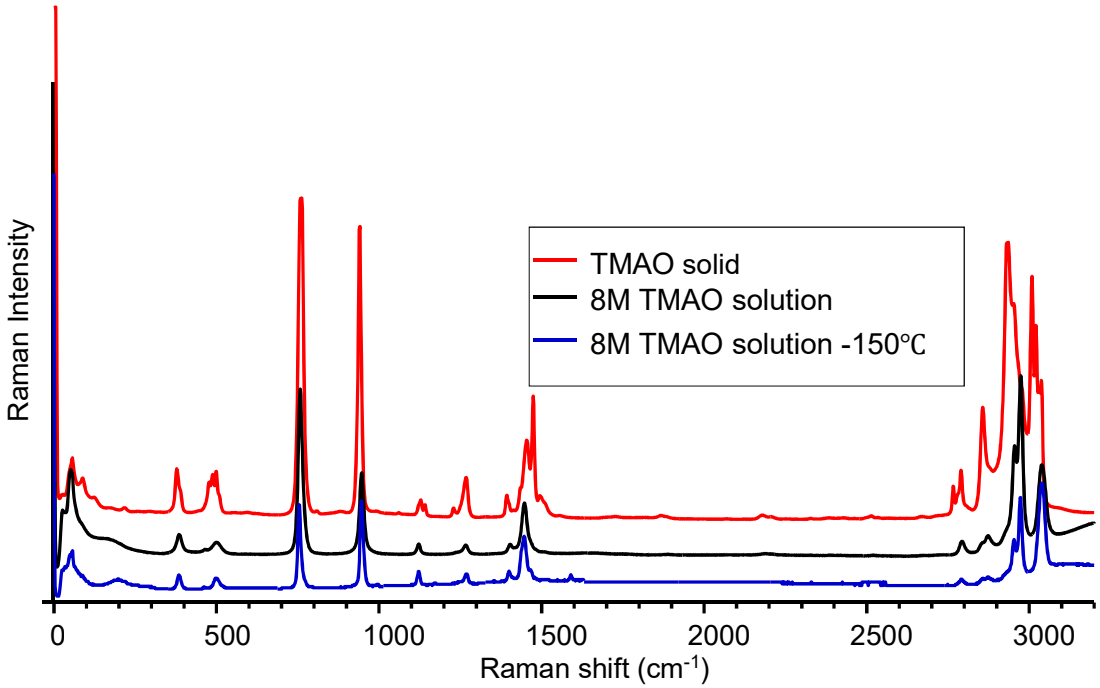

Figure 3.4.3: Raman spectral comparison of TMAO using temperature-controlled Raman

Chapter 4: Conclusion

Raman spectroscopy and computational data was used to study the hydrogen bonding between urea, gdn-HCl, TMAO, and water. Raman spectra taken of urea matched that from previous research indicating that urea and TMAO directly interact with one another when placed in the same solution. The serial dilution for each osmolyte showed that the peak intensity was dependent upon the concentration of the osmolyte in solution. It was also found that the solution of TMAO and gdn-HCl exhibited similar shifts to the TMAO urea spectra. Two peaks in the HNH bending region were shown to shift to higher energy by $10cm^{-1}$. The shift is consistent with direct interaction of TMAO and gdn-HCl. The direct interactions thus suggest that TMAO may counteract gdn-HCl's tendency to denature proteins.

Chapter 5: Future Work

There is a lot of possibilities for future work and applications to the above research. More theoretical data could be collected to make the spectra of the experimental match that of the theoretical with a higher affinity. Another addition to this research is the collection of data using different techniques including SERS and RUNS. The RUNS would expand on the concept of the TCS allowing the user to freeze the solutions. The lower temperature would lock the molecules into place restricting their movement and allowing for better resolution and peak separation when collecting Raman data.

Future work could also investigate studying different systems and system combinations. There are many more osmolytes out there along with kosmotropic and chaotropic agents. Raman data can be collected using different combinations of solutes and solvents to better understand both hydrogen bonding and protein interactions.

Another future research plan could investigate studying the crystal lattice structures of urea and urea in solution. The Raman spectrum taken at low temperature showed great potential because of the various perturbations that occurred in the spectrum.

Chapter 6: Forensic Chemistry Application

In its simplest form, a forensic chemist analyzes physical evidence found at a crime scene to assist in solving a crime. They do this by identifying and characterizing different types of evidence including blood, trace evidence, bodily fluids, mysterious powders, etc. Currently, DNA typing is the predominant means of identification of individuals. DNA does have its weakness and one of those is that is can be easily degraded especially once outside the body.[43] Proteins are more robust than DNA and contain single nucleotide polymorphism. A recent study looked at using proteins located in the hair shaft to correctly identify and distinguish different individuals. [44] By understanding how proteins interacts in different aqueous environments can lead to the increased use of proteins in a forensic chemistry setting. Understanding why proteins denature and renature can be used in the sample preparation of proteins for use in the discrimination of different individuals.

REFERENCES

1. Tro, N.J., *Chemistry: Structure and Properties*2015: Pearson Education.
2. Hobza, P. and Z. Havlas, *Blue-Shifting Hydrogen Bonds.* Chemical Reviews, 2000. **100**(11): p. 4253-4264.
3. Wright, A.M., et al., *Charge Transfer and Blue Shifting of Vibrational Frequencies in a Hydrogen Bond Acceptor.* The Journal of Physical Chemistry A, 2013. **117**(26): p. 5435-5446.
4. Yancey, P.H., et al., *Living with Water Stress: Evolution of Osmolyte Systems.* Science, 1982. **217**(4566): p. 1214-1222.
5. Burg, M.B. and J.D. Ferraris, *Intracellular Organic Osmolytes: Function and Regulation.* The Journal of Biological Chemistry, 2008. **283**(12): p. 7309-7313.
6. Street, T.O., D.W. Bolen, and G.D. Rose, *A molecular mechanism for osmolyte-induced protein stability.* Proceedings of the National Academy of Sciences of the United States of America, 2006. **103**(38): p. 13997-14002.
7. *Urea*. March 31 2018 [cited 2018 April 7]; Available from: https://pubchem.ncbi.nlm.nih.gov/compound/1176.
8. Wöhler, F., *Ueber künstliche Bildung des Harnstoffs.* Annalen der Physik, 1828. **88**(2): p. 253-256.
9. Nelson, D.L. and M.M. Cox, *Lehninger Principles of Biochemistry*. 6 ed2013, New York: W. H. Freeman.
10. *Guanidine Hydrochloride*. 2005 March 31 2018 [cited 2018 April 7]; Available from: https://pubchem.ncbi.nlm.nih.gov/compound/5742.
11. *Guanidinium*. 2004 March 31 2018 [cited 2018 April 7]; Available from: https://pubchem.ncbi.nlm.nih.gov/compound/32838.
12. *Tr-methylamine Oxide*. 2004 March 3 2018; Available from: https://pubchem.ncbi.nlm.nih.gov/compound/1145.
13. Velasquez, M.T., et al., *Trimethylamine N-Oxide: The Good, the Bad and the Unknown.* Toxins, 2016. **8**(11): p. 326.
14. Berg, J.M., J.L. Tymoczko, and L. Stryer, *Chapter 3: Protein Structure and Function*, in *Biochemistry*2002, W. H. Freeman: New York.
15. Stirling, P.C., V.F. Lundin, and M.R. Leroux, *Getting a grip on non-native proteins.* EMBO Reports, 2003. **4**(6): p. 565-570.
16. Stirnemann, G., et al., *How force unfolding differs from chemical denaturation.* Proceedings of the National Academy of Sciences of the United States of America, 2014. **111**(9): p. 3413-3418.
17. Wang, C., et al., *The structural basis of urea-induced protein unfolding in β-catenin.* Acta Crystallographica Section D: Biological Crystallography, 2014. **70**(11): p. 2840-2847.
18. Stumpe, M.C. and H. Grubmüller, *Aqueous Urea Solutions: Structure, Energetics, and Urea Aggregation.* The Journal of Physical Chemistry B, 2007. **111**(22): p. 6220-6228.
19. Wei, H., Y. Fan, and Y.Q. Gao, *Effects of Urea, Tetramethyl Urea, and Trimethylamine N-Oxide on Aqueous Solution Structure and Solvation of Protein Backbones: A Molecular Dynamics Simulation Study.* The Journal of Physical Chemistry B, 2010. **114**(1): p. 557-568.
20. Hoccart, X. and G. Turrell, *Raman spectroscopic investigation of the dynamics of urea–water complexes.* The Journal of Chemical Physics, 1993. **99**(11): p. 8498-8503.

21. Bennion, B.J. and V. Daggett, *The molecular basis for the chemical denaturation of proteins by urea.* Proceedings of the National Academy of Sciences of the United States of America, 2003. **100**(9): p. 5142-5147.
22. Braz, A., M. López-López, and C. García-Ruiz, *Raman spectroscopy for forensic analysis of inks in questioned documents.* Forensic Science International, 2013. **232**(1): p. 206-212.
23. Barone, G., E. Rizzo, and V. Vitagliano, *Opposite effect of urea and some of its derivatives on water structure.* Journal of Physical Chemistry, 1970. **74**(10): p. 2230-2232.
24. Alonso, D.O.V. and K.A. Dill, *Solvent Denaturation and Stabilization of Globular Proteins.* Biochemistry, 1991. **30**(24): p. 5974-5985.
25. Rashid, F., S. Sharma, and B. Bano, *Comparison of guanidine hydrochloride (GdnHCl) and urea denaturation on inactivation and unfolding of human placental cystatin (HPC).* Protein Journal, 2005. **24**(5): p. 283-292.
26. Gabel, D., *The Denaturation by Urea and Guanidinium Chloride of Trypsin and N-Acetylated-Trypsin Derivatives Bound to Sephadex and Agarose.* European Journal of Biochemistry, 1973. **33**(2): p. 348-356.
27. Munroe, K.L., D.H. Magers, and N.I. Hammer, *Raman Spectroscopic Signatures of Noncovalent Interactions Between Trimethylamine N-oxide (TMAO) and Water.* The Journal of Physical Chemistry B, 2011. **115**(23): p. 7699-7707.
28. Cuellar, K.A., et al., *Noncovalent Interactions in Microsolvated Networks of Trimethylamine N-Oxide.* The Journal of Physical Chemistry B, 2014. **118**(2): p. 449-459.
29. Travis, S.G., et al., *Noncovalent Interactions between Trimethylamine N-oxide (TMAO), Urea, and Water.*
30. Robinson, J.W., E.M.S. Frame, and G.M.F. II, *Undergraduate Instrumental Analysis*. 7 ed2014: CRC Press.
31. Hanania, J., K. Stenhouse, and J. Donev. *Ultraviolet Radiation*. [cited 2018 April 1]; Available from: http://energyeducation.ca/encyclopedia/Ultraviolet_radiation.
32. Engel, T. and P. Reid, *Physical Chemistry*. 3 ed2013: Pearson.
33. Libretexts. *The Molecular Interpretation of Entropy*. 2017 October 15, 2017 [cited 2018 April 1]; Available from: https://chem.libretexts.org/Textbook_Maps/General_Chemistry_Textbook_Maps/Map%3A_Chemistry%3A_The_Central_Science_(Brown_et_al.)/19%3A_Chemical_Thermodynamics/19.3%3A_The_Molecular_Interpretation_of_Entropy.
34. Andrews, D.L., *Molecular Photophysics and Spectroscopy*2014, San Rafael California: Morgan & Claypool Publishers.
35. II, R.M.G., et al., *Instrumental Analysis*2017, New York, New York: Oxford University Press. 846.
36. Hargreaves, M.D., et al., *Analysis of seized drugs using portable Raman spectroscopy in an airport environment—a proof of principle study.* Journal of Raman Spectroscopy, 2008. **39**(7): p. 873-880.
37. Miller, J.V. and E.G. Bartick, *Forensic Analysis of Single Fibers by Raman Spectroscopy.* Applied Spectroscopy, 2001. **55**(12): p. 1729-1732.
38. Virkler, K. and I.K. Lednev, *Raman spectroscopy offers great potential for the nondestructive confirmatory identification of body fluids.* Forensic Science International, 2008. **181**(1): p. e1-e5.
39. Raman, C.V. and K.S. Krishnan, *A New Type of Secondary Radiation.* Nature, 1928. **121**: p. 501.
40. Long, D.A., *The Raman Effect: A Unified Treatment of the Theory of Raman Scattering by Molecules*2002: John Wiley & Sons.

41. Keuleers, R., et al., *Vibrational Analysis of Urea.* The Journal of Physical Chemistry A, 1999. **103**(24): p. 4621-4630.
42. Grdadolnik, J. and Y. Maréchal, *Urea and urea–water solutions—an infrared study.* Journal of Molecular Structure, 2002. **615**(1): p. 177-189.
43. Butler, J., *Fundamentals of Forensic DNA Typing*. 1 ed2009: Academic Press.
44. Parker, G.J., et al., *Demonstration of Protein-Based Human Identification Using the Hair Shaft Proteome.* PLOS ONE, 2016. **11**(9): p. e0160653.